Electronic Supplementary Material (ESI) for Polymer Chemistry
This journal is © The Royal Society of Chemistry 2013

Electronic Supplementary Information

# Grafting of copolymers onto graphene by miniemulsion polymerization for conductive polymer composites: Improved electrical conductivity and compatibility induced by interfacial distribution of graphene

**Yeqiang Tan, Lijun Fang, Jianliang Xiao, Yihu Song* and Qiang Zheng***

# Experimental section

## Materials

Graphite (99.8%) with an average particle size of 45 μm was obtained from Alfa Aesar Co. Ltd., UK. Concentrated sulfuric acid ($H_2SO_4$), concentrated hydrochloric acid (HCl), potassium persulfate ($K_2S_2O8$), phosphorus pentoxide ($P_2O_5$), potassium permanganate ($KMnO_4$), sodium nitrate ($NaNO_3$), hydrogen peroxide ($H_2O_2$, 30%), hydrazine hydrate (85%), γ-methacryloxy-propyl trimethoxysilane (MPS), 2,2'-azobisisobutyronitrile (AIBN), hexadecane (HD), polyoxyethylene nonylphenyl ether (OP-10), divinyl benzene (DVB), sodium dodecyl benzene sulfonate (SDBS), sodium bicarbonate ($NaHCO_3$), ethanol, tetrahydrofuran and dimethylformamide of analytical purity were purchased from Shanghai Chem. Reagent Co. Ltd., China. All the materials were used without further purification. Styrene (St) and methylmethacrylate (MMA) (Hangzhou Chem. Reagent, China) was distilled under reduced pressure and stored at -30 °C before use. Polystyrene (PS) (680A, $M_w = 1.9\times10^5$, $M_w/M_n = 2.05$, Dow Chem Co. Ltd, USA) and poly(methyl methacrylate) (PMMA) (IF850, $M_w = 8.1\times10^4$, $M_w/M_n = 1.9$, LG Co. Ltd., South Korea) were commercial products and were used as received.

## Preparation of graphene oxide nanosheets

Graphene oxide (GO) was synthesized from natural graphite powder using a modified Hummers' method [1,2] including two steps of oxidation. In the pre-oxidation step, $K_2S_2O_8$ (8.4g) and $P_2O_5$ (8.4 g) were dissolve in concentrated $H_2SO_4$ (40 mL) at 80 °C, followed by slow addition of graphite powder (10 g). The oxidation reaction was conducted at 80 °C for 4.5 h. After cooling down to room temperature, the suspension was diluted with deionized water and laid overnight. The mixture was then vacuum-filtered and washed with deionized water (1.5 L) using a 0.22 μm polycarbonate membrane. The product obtained was dried in air at room temperature. In the second oxidation step, the pretreated graphite powder was poured into concentrated $H_2SO_4$ (230 mL) in an ice bath and stirred until the temperature dropped to 0-3 °C. $KMnO_4$ (60 g) was added gradually under continuous stirring, and the temperature was kept below 10 °C. The mixture was then heated to 35 °C and stirred for 2 h, followed by diluting with deionized water (0.5 L) and further stirring for 30 min. The reaction was terminated by adding deionized water (1.5 L) and 30 % $H_2O_2$ (25 mL). The mixture was left undisturbed for 2 days and the nearly clear supernatant was decanted. The lower precipitate was filtered and washed with 1 M HCl solution to remove residual metal oxides. The products were subjected to cycles of water-washing and separation via centrifugation until pH value of the decantate reached 6. The sample of GO was obtained after freeze-dehydration for 2 days and after vacuum-drying for 24 h.

## Synthesis of MPS-modified GO

GO powders (400 mg) were dispersed in 200 ml deionized water and the suspendiosn was treated with ultrasound for 30 min, yielding completely exfoliated GO nanpsheet suspension. Then, MPS was added into the as-prepared GO dispersion and the reaction solution was adjusted to a pH value of 4.5 using HCl. The hydrolysis of MPS and condensation of GO were carried out simultaneously at 60 °C for 12 h to produce the functionalized GO solution.[3] The methoxy groups of MPS hydrolyze readily in aqueous solvents to form silanol groups (Equation S1), and self-condensation of the silanol to insoluble polysiloxane was likely to occur, greatly hindering the condensation between the silanol groups and the hydroxyl groups on the GO sheets (Scheme 1). Hydrolysis and condensation reactions of silane coupling agents in aqueous media are catalyzed by both acids and bases with the minimum hydrolysis reaction rate at pH 7 and the minimum self-condensation reaction rate at pH 4.5.[4,5] Thus, the experimental condition (pH 4.5) facilitated the hydrolysis reaction while restrained the self-condensation reaction to ensure that a majority of silanol groups sufficiently condensed with hydroxyl groups on the GO sheets. The MPS modified GO (MPS-GO) was obtained by centrifugation (at 12000 rpm for 10 min) and redispersion in ethanol for 4 times. The brown deposit was dried to constant weight at 60 °C in vacuum for 24 h.

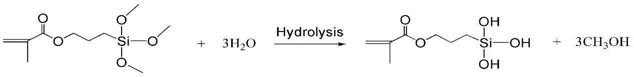

**Equation S1** Illustration of the hydrolysis of MPS.

## Synthesis of poly(styrene-*co*-methylmethacrylate) grafted GO sheets via miniemulsion polymerozation

All the components required in this procedure were divided into two parts. One was aqueous phase, which included 50 mL deionized water, 20 mg OP-10, and 100 mg SDBS. The other was oil phase, which composed of 5 g St, 5 g MMA, 5 g hexadecane, 100 mg MPS-GO,100 mg HD, 100 mg AIBN, and 0.02 g DVB. The oil phase without AIBN was mixed for 10 min by stirring and was ultrasonicated in an ice bath for 10 min to obtain a homogenous dispersion. Then AIBN was dissolved in the oil phase. The oil phase was added to the aqueous phase and the O/W mixture was mixed for 30 min by magnetic stirring for pre-emulsification. The O/W mixture was ultrasonicated using a ultrasonicator (JY92-II Sonifier, Ningbo Xinzhi, China) in an ice bath for 20 min (output power 500 W, work time

2 s, pause time 6 s). The miniemulsion was then stirred for 30 min in order to homogenize the system. The miniemulsion was poured into 100 mL three-necked glass reactor equipped with condenser and mechanical stirrer in an oil bath. The reaction was carried out at 70 °C for 2 h under stirring rate 300 rpm. After polymerization, the product was demulsificated and purified from emulsifier by centrifugation (at 3000 rpm for 10 min) and redispersion in 60 °C deionized water for 4 times. The acquired product included poly(styrene-*co*-methylmethacrylate) grafted GO sheets (P(St-*co*-MMA)-*g*-GO) and free P(St-*co*-MMA). DMF was used to dissolve the free P(St-*co*-MMA). Undissolved products were collected by centrifugation and were subsequently dried at 60 °C in vacuum for 24 h. Finally, a harsh extraction with boiling tetrahydrofuran for 72 h was carried our to completely remove free copolymers.

### Preparation of P(St-*co*-MMA)-*g*-RGO/PS/PMMA composites

Certain amounts of powder were dispersed in DMF and treated with ultrasound for 30 min, yielding completely exfoliated GO sheet suspension. PS and PMMA with certain volume ratios (1/1 and 4/1) were dissolved in DMF for 2 h. The P(St-*co*-MMA)-*g*-GO dispersion was gradually added to the polymer solution under magnetic agitation and the suspension was sonicated for an additional 30 min. To prepare P(St-*co*-MMA)-*g*-RGO/PS/PMMA suspensions, hydrazine was added to the as-prepared P(St-*co*-MMA)-*g*-GO/PS/PMMA suspensions under magnetic agitation for 30 min. GO was reduced to RGO by refluxing the mixture at 95 °C for 8 h. After reduction, the mixture dispersion was coagulated with methanol under vigorous stirring. The black solid products (P(St-*co*-MMA)-*g*-RGO/PS/PMMA composites) were filtered, washed with abundant methanol, and vacuum-dried at 50 °C overnight. The contrast composites filled with unmodified RGO were obtained by exactly the same procedure.

### Characterizations

Atomic force microscopy (AFM) tapping-mode images were taken on NSK SPI3800 (NSK Co. Ltd., Japan). The samples were prepared by spin-coating the solutions onto freshly exfoliated mica substrates. X-ray diffraction (XRD) was carried out using a Rigaku X-ray generator equipped with Cu K$\alpha$ radiation ($\lambda$ = 0.154 nm) (Rigaku Co. Ltd., Japan). Fourier-transform infrared (FTIR) spectra were recorded with a spectrometer (Vector 22, Bruker, Germany) using KBr pellet technique. Grafting ratio of copolymer onto GO nanosheets was evaluated by thermogravimetry analysis (TGA, Q1000, TA, USA) at a heating rate of 5 °C min$^{-1}$ under nitrogen. Particle size distributions of latex were obtained by laser dynamic light scattering (DLS; BI-90 plus, Brookhaven Instruments, USA) in $H_2O$ at 50 °C (scattering angle 90 °). Molecular weight of the polymers was measured by size exclusion chromatography (SEC, Aligent 1100 HPLC, America) equipped with a 79911GP-MXC column and a RI detector at 25 °C in tetrahydrofuran solution at an elution rate of 1.0 mL min$_{-1}$ against PS standards. Proton nuclear magnetic resonance ($^1$H NMR) spectra was recorded on a Bruker DMX-500 spectrometer (Brulcer, Switzerland) with tetramethylsilane as internal standard and $CDCl_3$ as solvent. Transmission electron microscope (TEM, JEM-1200EX, JEOL, Japan) was employed to investigate the morphology of latex and the distribution of sheets in composites. The latex samples were prepared by casting one drop of a dilute suspension onto a copper grid; and the composite samples were microtomed into sections of 100 nm thick for TEM observation. The phase morphology was observed under a scanning electron microscope (SEM, S4800, Hitachi, Japan) at an acceleration voltage of 3 kV. The average size of dispersed phase was calculated from the SEM pictures with the aid of computer software (ImageJ Version 1.45). For preparing the SEM samples, specimens were first fractured in liquid nitrogen. Then the PMMA phase was etched by formic acid and the remained sample was sputter-coated with a thin layer of gold.

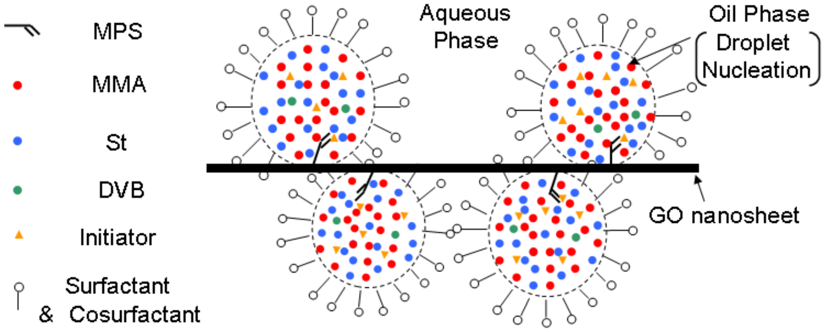

**Scheme S1** Schematic illustration of the miniemulsion system after pre-emulsification by mixing the oil phase containing MPS-GO and the aqueous phase *via* intensive ultrasound. MPS-GO previously dispersed in the oil phase was initially sufficiently infiltrated by monomers and initiators. After pre-emulsification, a large section of the hydrophilic GO nanosheets were immersed in aqueous phase while the grafted MPS with polymerizable double bond was encapsulated by hydrophobic monomers and initiators to constitute submicrometer droplets stabilized by the surfactant and the cosurfactant. Thus, droplet nucleation is the predominant mechanism of miniemulsion formation in the polymerization step due to the small size of the monomer droplets and the presence of few or no micelles in the system; the adoption of hydrophobic initiators also greatly prevents the occurrence of homogeneous nucleation.

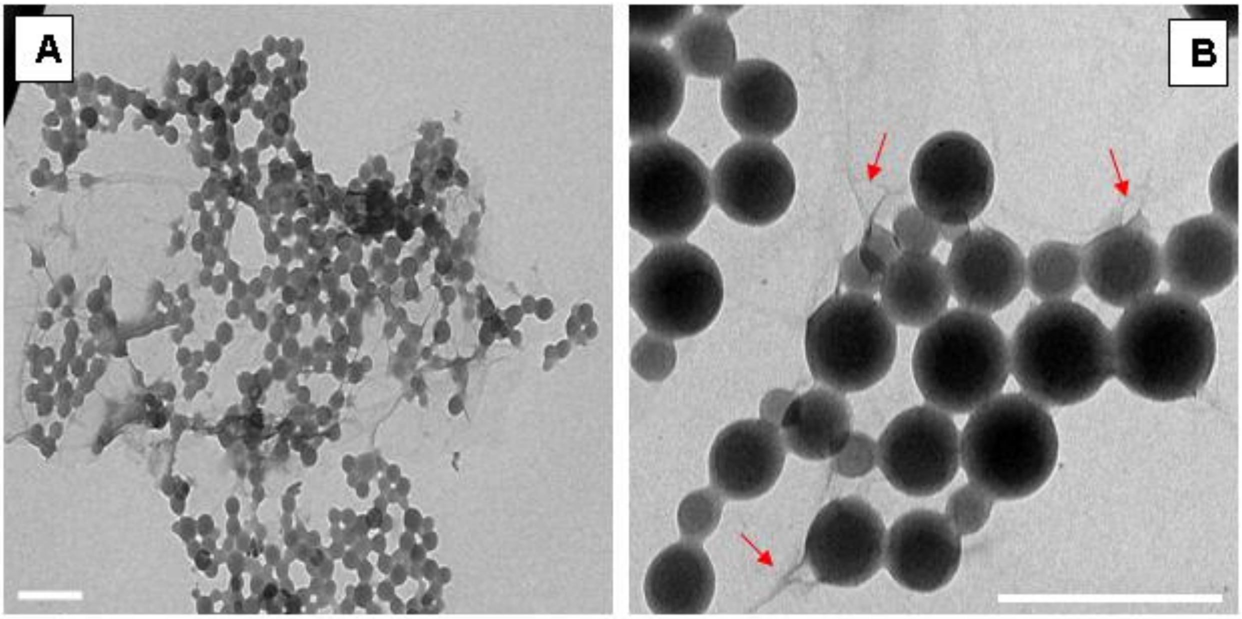

**Fig. S1** TEM images of P(St-co-MMA)-*g*-GO latex diluted three times under low (A) and high magnifications (B). The scale bars represent 0.5 $\mu$m. The small red arrows point to the folds and edges of the crumpled and transparent GO nanosheets.

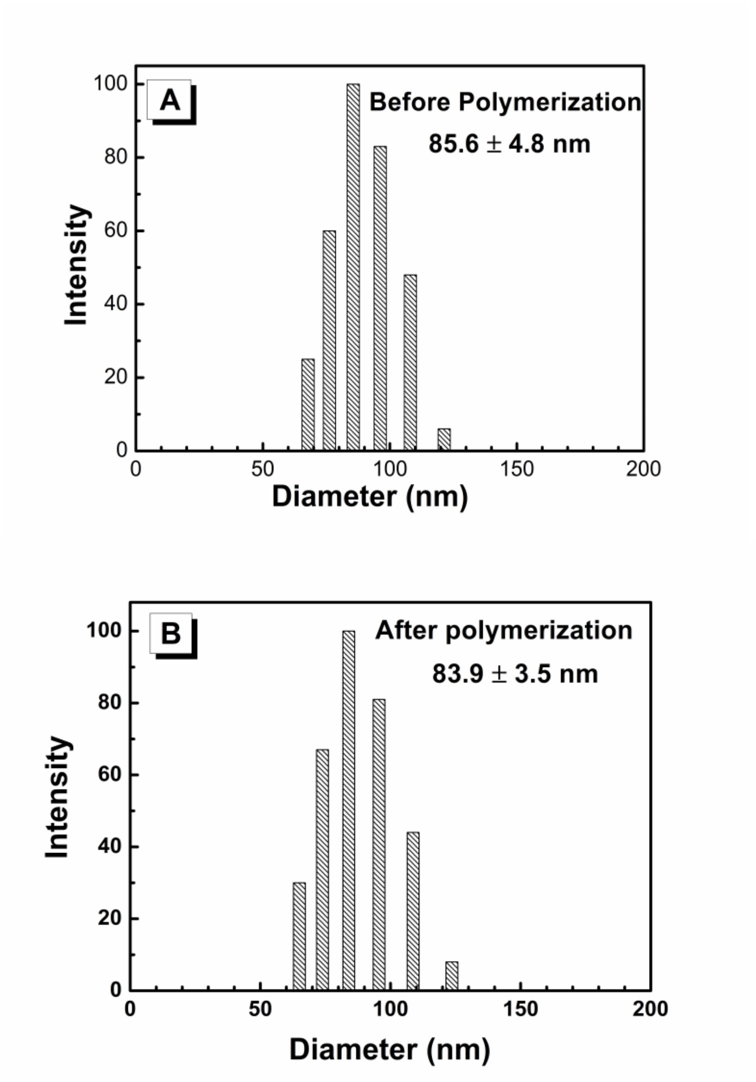

**Fig. S2** Particle size distributions of P(St-*co*-MMA)-*g*-GO latex before (A) and after (B) miniemulsion polymerization obtained by DLS. Both of them exhibit narrow size distributions. Noting that almost the same latex sizes before and after polymerization reveal that the miniemulsion droplets are directly polymerized to polymer particles via droplet nucleation.[6-7]

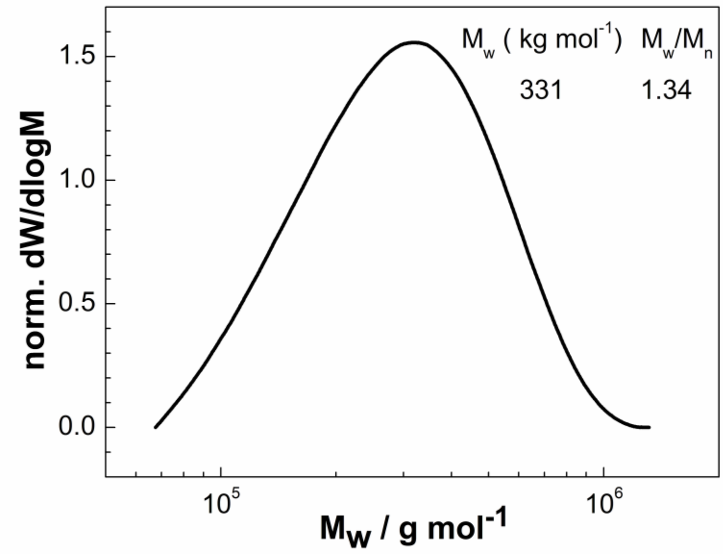

**Fig. S3** Molecular weight distribution of free P(St-*co*-MMA) using SEC. Weight averaged molecular weight ($M_w$) and polydispersity index ($M_w/M_n$) are determined as $3.31\times10^5$ and 1.34, respectively. The narrow molecular weight distribution was precisely the manifestation of uniform particle size and regular structure in miniemulsion polymerization process.[7]

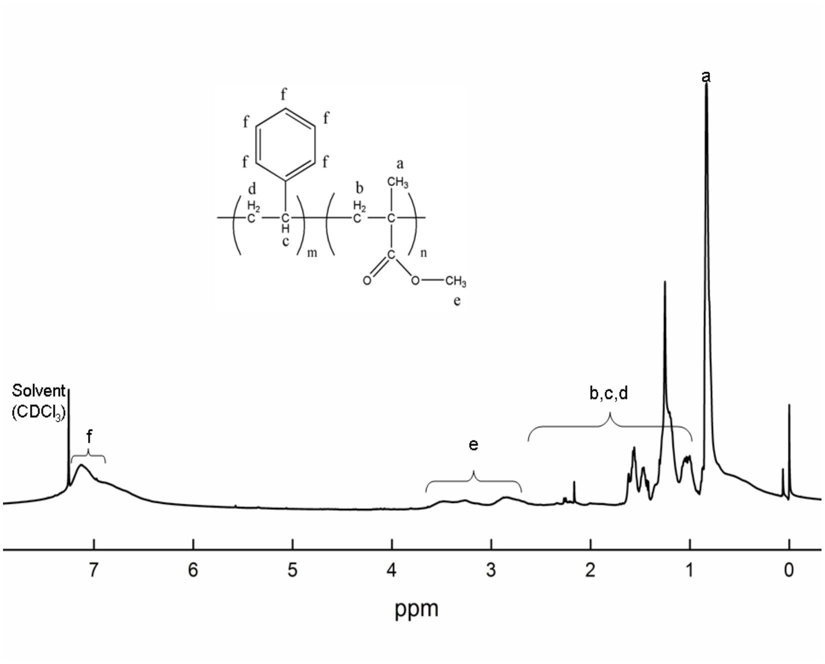

**Fig. S4** $^1$H-NMR spectrum of the free P(St-*co*-MMA). Given that miniemulsion copolymerization with empirical monomer reactivity ratios of $r_m = 0.46$ for MMA and $r_s = 0.52$ for St is a conventional radical copolymerization in essence, adduct radicals do not incline to react with a specific comonomer and thus a random P(St-*co*-MMA) copolymer is generated as has been widely proved.[8-11] The one-step feeding with a feed ratio of [50]:[50] in our study also promotes the production of a random copolymer.[9] Meanwhile, as shown in $^1$H-NMR spectrum, many split overlapping peaks at 0.93-1.65 ppm and rather broad peaks at 2.5-3.6 ppm are assigned to protons in the backbone (b, c, d) and methoxy-H (e) in the side chain, respectively, which are more complicated than that of the corresponding block and alternating copolymer.[10-11] There possibly is a wide variety of sequence distribution and the produced P(St-*co*-MMA) by miniemulsion polymerization possess a random sequence distribution on the basis of theoretical analysis together with experimental results. [8-11]

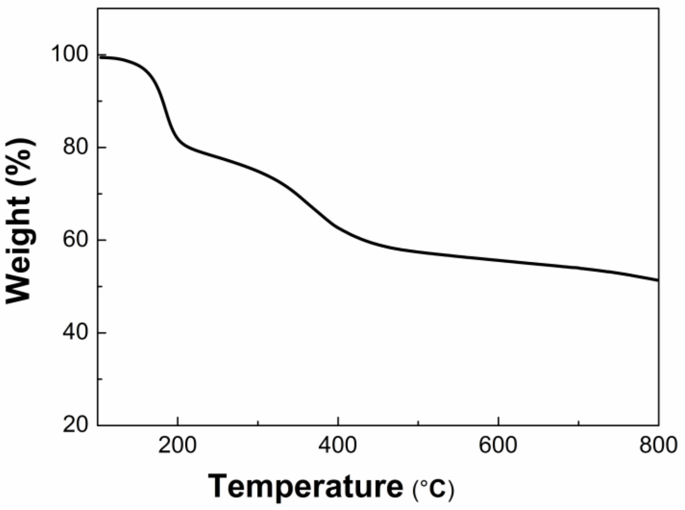

**Fig. S5** TGA curve of P(St-*co*-MMA) modified GO without DVB. TGA data for unmodified GO showed a 43.0% weight loss in a nitrogen atmosphere at 800 °C (Fig. 2B), whereas modified GO without DVB and free P(St-*co*-MMA) had a weight losses of 48.6 and 99.0%, respectively. Therefore, the quantity of grafted copolymers in modified GO without DVB is estimated as ca 9.8 wt % being far less than that of P(St-*co*-MMA)-*g*-GO, which proves that a very small amount (0.2 wt% relative to monomer) of DVB in the miniemulsion system effectively increases grafting rate of P(St-*co*-MMA) onto GO.

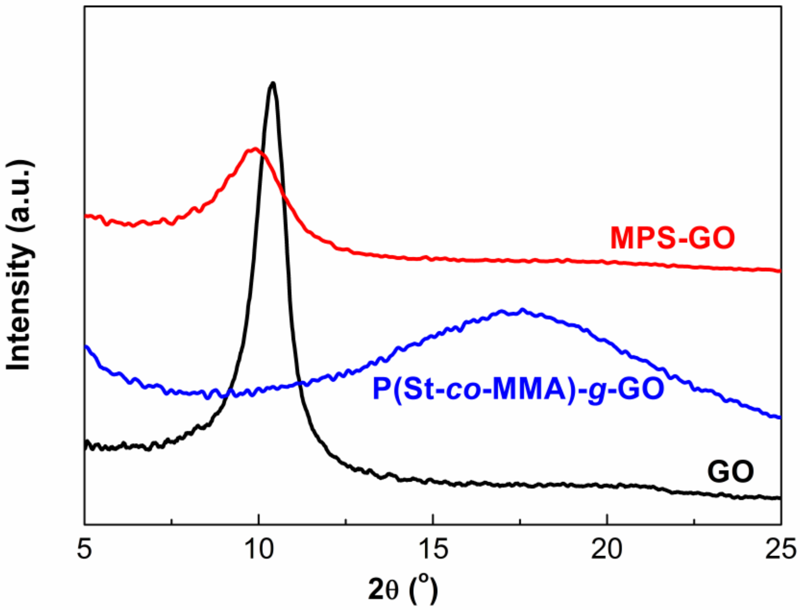

**Fig. S6** XRD patterns of GO, MPS-GO, and P(St-*co*-MMA)-*g*-GO powders. GO exhibits a sharp diffraction peak at $2\theta$ = 10.4° corresponding to a layer-to-layer distance of 0.85 nm according to Bragg's law. A diffraction peak of MPS-GO appears at $2\theta$ = 9.8°, representing an interlayer spacing of 0.89 nm due to intercalation by grafted MPS between GO sheets. P(St-*co*-MMA)-*g*-GO shows a broad and weak peak at $2\theta$ = 17° without appearance of the characteristic low-angle peaks, which can be ascribed to exfoliation into a monolayer or few-layers[12] accompanying with a high grafting ratio of P(St-*co*-MMA) onto GO sheets.

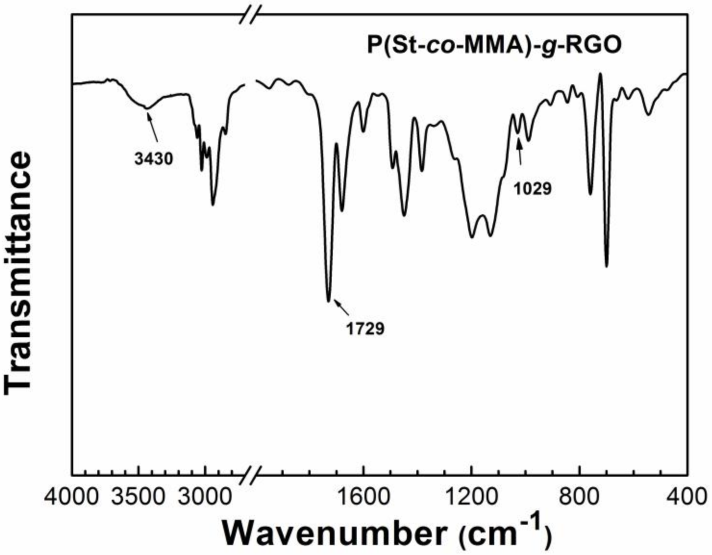

**Fig. S7** FTIR spectrum of P(St-*co*-MMA)-*g*-RGO. Absorption bands at 3430 cm$^{-1}$ and 1029 cm$^{-1}$ corresponding to stretching vibrations of hydroxyl and epoxy groups were significantly reduced in comparison with that of P(St-*co*-MMA)-*g*-GO (Fig. 1), indicating the effective GO reduction by hydrazine hydrate.

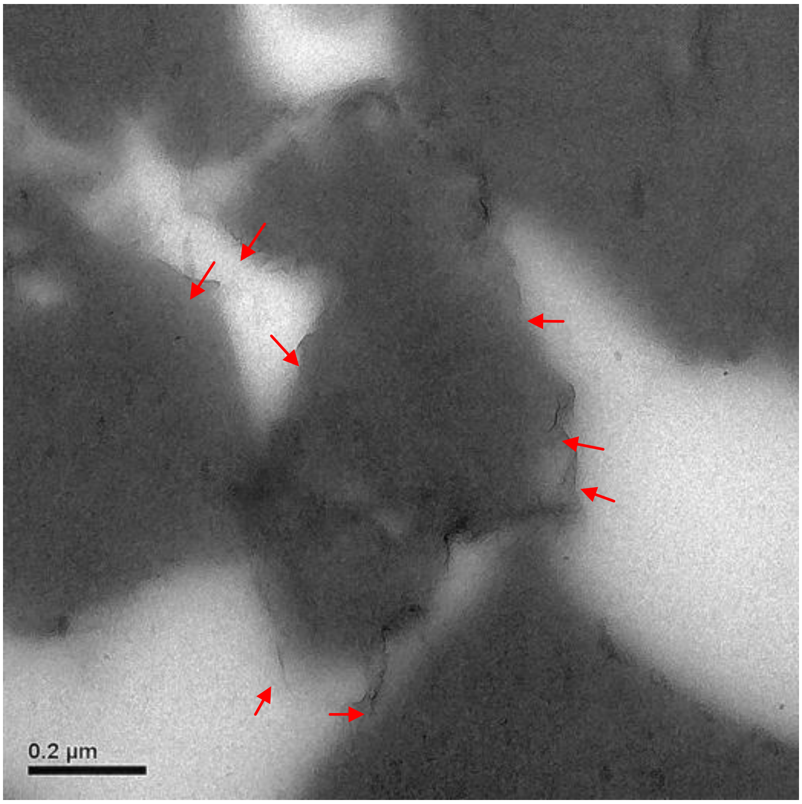

**Fig. S8** TEM images of P(St-*co*-MMA)-*g*-RGO filled PS/PMMA (1/1 in volume) blend at 0.46 vol% RGO loading. The small red arrows point to the recognized RGO nanosheets. Graphene nanoplatelets of 2-5 nm in thickness corresponding to 2-5 layers stacking are distributed at the interface between PS and PMMA phases. Most of the exfoliated RGO sheets are dispersed as a thin layer in the polymer matrix due to strong interactions between P(St-*co*-MMA)-*g*-RGO sheets with both the two phases.

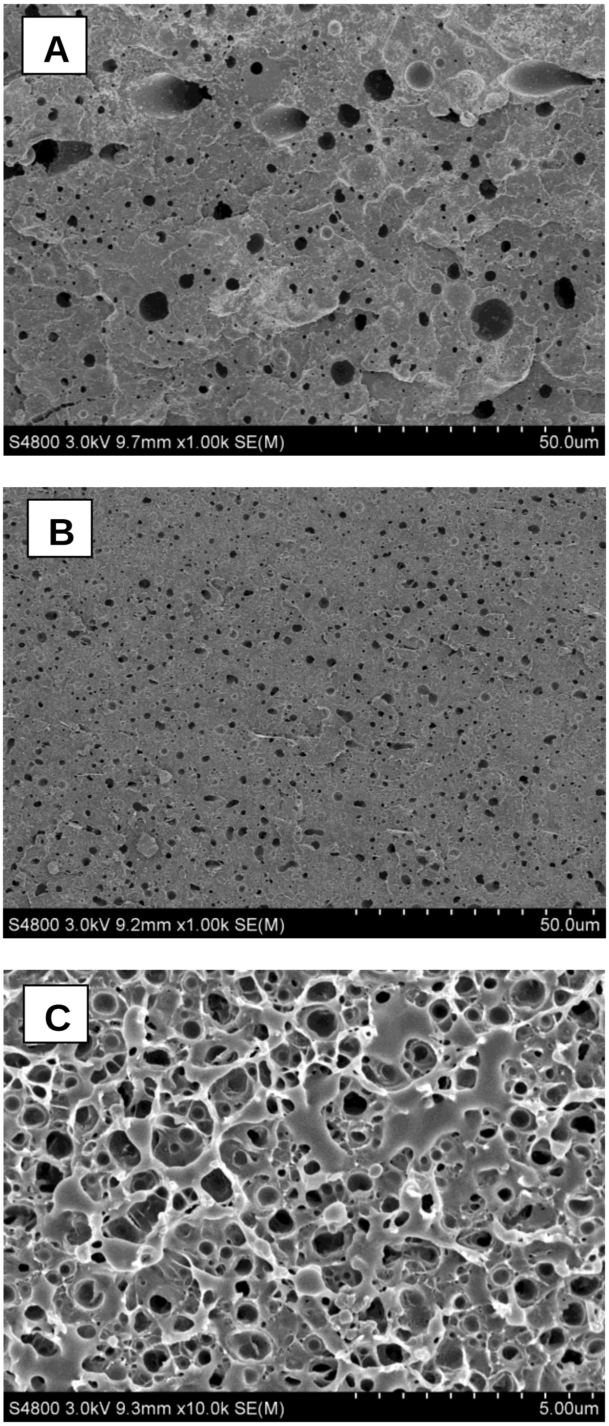

**Fig. S9** SEM images of unfilled (A) and RGO (B) and P(St-*co*-MMA)-*g*-RGO filled PS/PMMA (4/1 in volume) blends (C) at 0.46 vol% RGO loading. All the images are used for measuring the size of PMMA phase. The rather large holes in Fig. S9A represent the greatly agglomerated PMMA phase due to the bad compatibility between PMMA and PS.

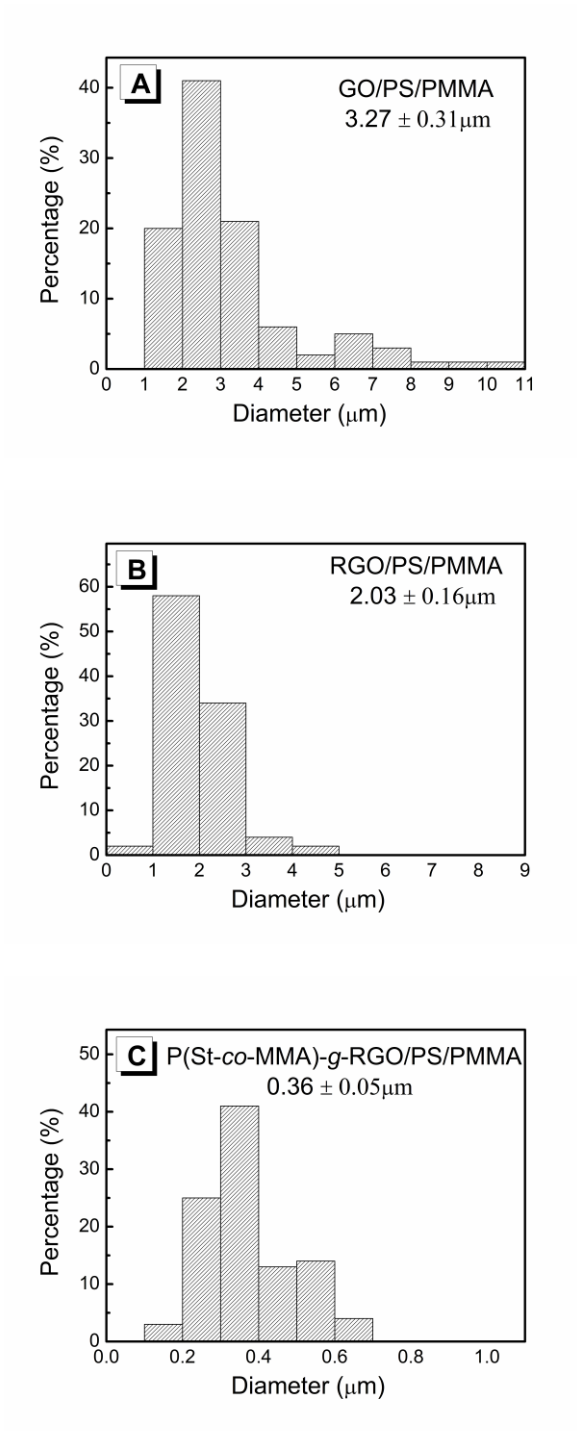

**Fig. S10** Size distribution histograms of unfilled (A) and RGO (B) and P(St-*co*-MMA)-*g*-RGO filled PS/PMMA (4/1 in volume) blends (C) at 0.46 vol% RGO loading calculated from Fig. S9 with the aid of ImageJ.

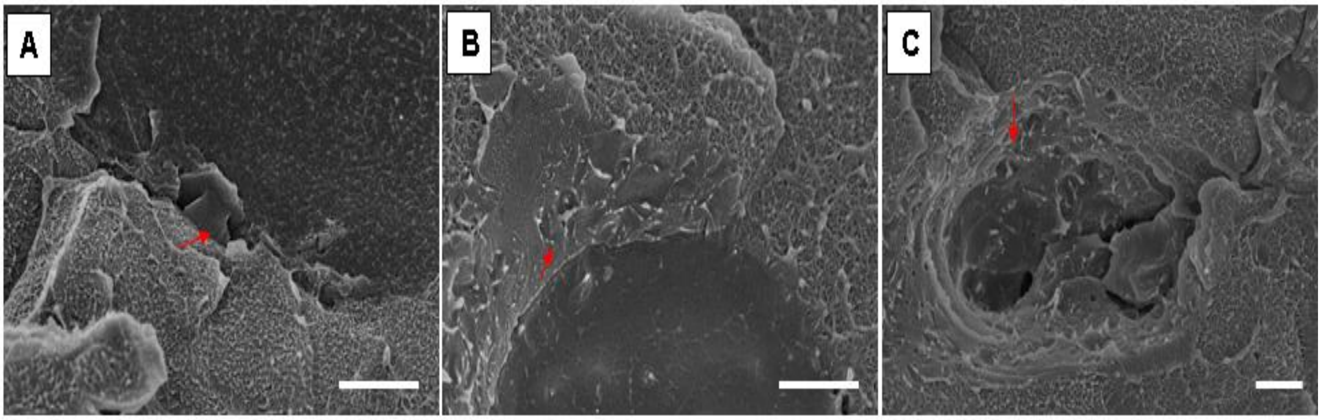

**Fig. S11** SEM images of P(St-*co*-MMA)-*g*-RGO filled PS/PMMA (4/1 in volume) blend at 0.46 vol% RGO loading under high magnification. The scale bars represent 0.1 $\mu$m. The blend was not etched by formic acid. The small red arrows point to the RGO nanosheets dispersed at the PS/PMMA interface of the blends. The immiscible phases are linked by RGO sheets at the interface, which is responsible for the considerably reduced phase size shown in Fig. S10.

# Reference

1 W. S. Hummers and R. E. Offeman, *J. Am. Chem. Soc.*, 1958, **80**, 1339-1339.
2 Y. Q. Tan, Y. H. Song and Q. Zheng, *Nanoscale*, 2012, **4**, 6997–7005.
3 J. C. Wang, C. H. Xu, H. T. Hu, L. Wan, R. Chen, H. Zheng, F. M. Liu, M. Zhang, X. P. Shang and X. B. Wang, *J. Nanopart. Res*., 2011, **13**, 1869-878.
4 M. W. Daniels, J. Sefcik, L. F. Francis, and A. V. McCormick, *J. Colloid. Interf. Sci.*, 1999, **219**, 351–356.
5 M. Iijima, M. Tsukada and H. Kamiya, *J. Colloid. Interf. Sci.*, 2007, **307**, 418–424.
6 K. Landfester, N. Bechthold, S. Forster and M. Antonietti, *Macromol. Rapid Commun.*, 1999, **20**, 81–84.
7 H. M. Etmimi and R. D. Sanderson, *Macromolecules*, 2011, **44**, 8504-8515.
8 Z. R. Guo, G. J. Yang, D. C. Wan and J. L. Huang, *J. Appl. Polym. Sci.*, 2001, **82**, 1472-1482.
9 M. A. Semsarzadeh and M. Abdollahi, Polymer, 2008, **49**, 3060-3069.
10Z. Wang, Q. Z. Dong and C. P. Hua, *Chinese J Polym Sci*, 2009, **27**, 367-374.
11 J.San Román, E.L. Madruga and M.A. del Puerto, *Angew. Makromol. Chem.*, 1980, **86**, 1-8.
12 S. Wang, Y. Zhang, N. Abidi and L. Cabrales, *Langmuir*, 2009, **25**, 11078-11081.